CHIN. PHYS. LETT. Vol. 34, No. 3 (2017) 037102

Anomalous Magneto-Transport Behavior in Transition Metal Pentatelluride $HfTe_5$ *

Ling-Xiao Zhao(赵凌霄)[1], Xiao-Chun Huang(黄筱淳)[1], Yu-Jia Long(龙雨佳)[1], Dong Chen(陈栋)[1], Hui Liang(梁慧)[1], Zhan-Hai Yang(杨占海)[1], Mian-Qi Xue(薛面起)[1], Zhi-An Ren(任治安)[1,2], Hong-Ming Weng(翁红明)[1,2]**, Zhong Fang(方忠)[1,2,3], Xi Dai(戴希)[1,2,3], Gen-Fu Chen(陈根富)[1,2,3]**

[1]*Institute of Physics and Beijing National Laboratory for Condensed Matter Physics, Chinese Academy of Sciences, Beijing 100190*

[2]*Collaborative Innovation Center of Quantum Matter, Beijing 100190*

[3]*School of Physical Sciences, University of Chinese Academy of Sciences, Beijing 100190*

(Received 9 December 2016)

There is a long-standing confusion concerning the physical origin of the anomalous resistivity peak in transition metal pentatelluride $HfTe_5$. Several mechanisms, such as the formation of charge density wave or polaron, have been proposed, but so far no conclusive evidence has been presented. In this work, we investigate the unusual temperature dependence of magneto-transport properties in $HfTe_5$. It is found that a three-dimensional topological Dirac semimetal state emerges only at around T_p (at which the resistivity shows a pronounced peak), as manifested by a large negative magnetoresistance. This accidental Dirac semimetal state mediates the topological quantum phase transition between the two distinct weak and strong topological insulator phases in $HfTe_5$. Our work not only provides the first evidence of a temperature-induced critical topological phase transition in $HfTe_5$ but also gives a reasonable explanation on the long-lasting question.

PACS: 71.30.+h, 73.43.Nq, 72.15.Gd, 81.10.Bk DOI: 10.1088/0256-307X/34/3/037102

The discovery of both two-dimensional (2D) and three-dimensional (3D) topological insulators (TIs) has attracted much attention in recent years due to their rich physics and promising applications in electronic and spintronic devices.[1–4] Recently, many of topological phases of matter, such as topological crystalline insulators,[5–8] topological Kondo insulators,[9–12] topological Dirac[13–17] and Weyl[18–25] semimetals (DSMs/WSMs), have been predicted theoretically and realized experimentally. These exotic topological quantum phases could also be tuned or induced by applying pressure, varying temperature or chemical substitution, etc.[26–32] For example, by fine tuning the chemical composition to the critical point of the topological phase transition between a normal insulator and a strong TI, the bulk band gap goes to zero at topological critical point (TCP) and the bulk band structure could be described by a 3D Dirac fermion state.[30,32]

Quasi-two-dimensional (Q2D) layered compound $HfTe_5$, previously known as a thermoelectric material, has stimulated extensive investigating interests for the pronounced resistivity peak occurring at around T_p = 50–90 K.[33–35] However, the origin of the mysterious transport feature has been an unsolved question for a long time.[33–37] Recent theoretical calculations predicted that single-layer $HfTe_5$ is a large gap quantum spin Hall insulator, and the bulk $HfTe_5$ with stacking of many layers locates in the vicinity of a transition between strong and weak TI.[38] This predication has renewed the interest in exploring its topological characters and unveiling the mystery of the origin of the anomalous resistivity peak. In this work, we study the temperature dependence of magneto-transport properties in $HfTe_5$, and find that the observed anomalous resistivity peak is intimately tied to a critical point. We show that, at around T_p, magnetoresistance (MR) exhibits an archetypal weak anti-localization (WAL) character in the perpendicular current and magnetic fields. When the magnetic field is rotated to parallel to the current, a chiral anomaly-resulted negative MR[39–44] is observed. Above or below T_p, however, the negative MR is suppressed gradually. All these results demonstrate clearly that, at around T_p, a 3D topological DSM state emerges, which mediates the topological quantum phase transition between the two distinct weak and strong TI phases in $HfTe_5$. At high temperatures, the bulk band gap is opened and $HfTe_5$ exhibits semiconducting behavior. With the sample cooling, the bulk band gap goes to zero at T_p and thereafter the surface state dominates the electronic transport properties, which thus leads to a pronounced resistivity peak at around T_p. The present finding provides a new perspective in further exploring the

*Supported by the National Basic Research Program of China under Grant Nos 2015CB921303 and 2013CB921700, the National Key Research Program of China under Grant No 2016YFA0300604, and the 'Strategic Priority Research Program (B)' of the Chinese Academy of Sciences under Grant No XDB07020100.

**Corresponding author. Email: gfchen@iphy.ac.cn; hmweng@iphy.ac.cn

© 2017 Chinese Physical Society and IOP Publishing Ltd

intriguing DSM/WSM states and gives a reasonable interpretation for the long-standing confusion of the pronounced resistivity peak in $HfTe_5$.

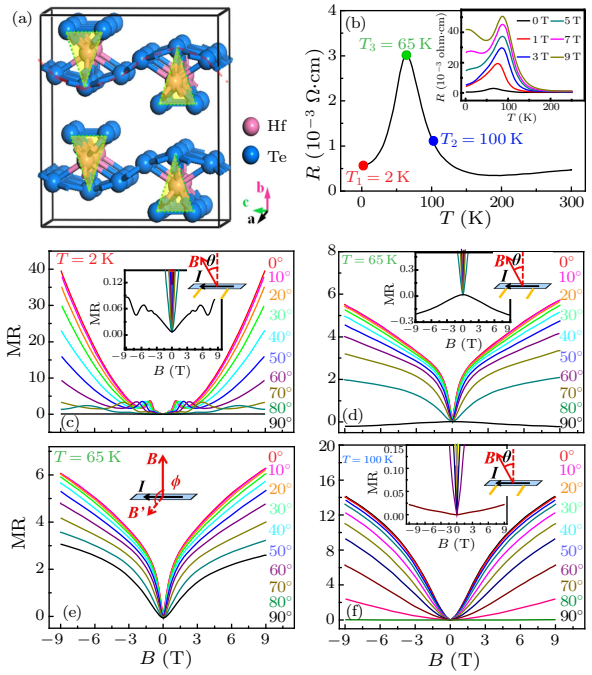

Fig. 1. (a) Crystal structure of $HfTe_5$ with $Cmcm$ (D_{2h}^{17}) space group. The yellow trigons highlight $HfTe_3$ chain which runs along the a-axis and linked via zigzag chains of Te atoms denoted by red dashed line. The main interaction between layers is van der Waals force. (b) Main panel: temperature-dependent resistivity in zero field. Three typical temperature points of $T = 2$, 65 and 100 K for further magneto-resistivity measurements are marked by red, green and blue, respectively. Inset panel: temperature-dependent resistivity in the fields of 1, 3, 5, 7 and 9 T. The applied magnetic fields not only significantly increase the resistivity, but also stimulate metallic-insulating transitions at low temperatures in definite strength. Magneto-resistance with applied field from perpendicular ($\theta = 0°$) to parallel ($\theta = 90°$) to the electric current at 2 K (c), 65 K (d) and 100 K (f), respectively. The insets zoom in on the lower MR parts and depict the corresponding measurement configurations. Here θ is defined as the angle between the magnetic field and the electric field. The negative MR and the WAL behavior appear at around 65 K the temperature of the anomalous resistivity peak. (e) Angular dependent MR at 65 K with keeping magnetic field perpendicular to electric current. The inset shows the measurement configuration. Here Φ is defined as the angle between $\boldsymbol{B}$ and $\boldsymbol{B}'$. The disappeared negative MR implied that it may stem from the topological $\boldsymbol{E}\cdot\boldsymbol{B}$ term.

Single crystals of $HfTe_5$ were grown by chemical vapor transport. Stoichiometric amounts of Hf (powder, 3N, Zr nominal 3%) and Te (powder, 5N) were sealed in a quartz ampoule with iodine (7 mg/mL) and were placed in a two-zone furnace. Typical temperature gradient from 500℃ to 400℃ was applied. After one month, long ribbon-shaped single crystals were obtained with the preferred direction of growth along the a-axis, as determined by face indexing using x-ray diffraction (XRD). The average stoichiometry was also determined by an energy-dispersive x-ray (EDX) spectroscopy. The magneto-resistance (MR) was measured with the four-point probe method in a quantum design PPMS, and the Hall coefficient measurement was carried out using a five-probe technique. Electrical contact was made using Au wires bonded to the crystal with Au paint. For MR (or Hall resistivity) measurements, any Hall (or resistive) voltages due to misalignment of the voltage leads could be corrected by reversing the direction of the magnetic field.

Figure 1(a) shows the crystal structure of $HfTe_5$, trigonal prismatic $HfTe_3$ chains run along the a-axis, and the largest natural facet determined by x-ray diffraction is the (010) plane which stacks along the b-axis. Theoretical calculations suggested that the interlayer interaction dominated by van der Waals (vdW) bonding is as weak as that of graphite.[38] Hence, to some extent, this system may be regarded as a Q2D electron system due to the weak interlayer coupling. The MR measurements are implemented on different samples by applying the current along the ribbon axis in a quantum design PPMS system. Figure 1(b) presents a typical temperature-dependent resistivity curve $\rho(T)$ in zero magnetic field, which shows a metallic behavior down to ∼175 K. However, with further decreasing temperature, $\rho(T)$ increases and reaches a maximum at around $T_p \sim 65$ K. Below 65 K, we observe the metallic-like behavior again with a nearly saturated resistivity at 2 K. This exotic phenomenon is investigated at various magnetic fields, as shown in the inset of Fig. 1(b). The applied magnetic fields significantly increase the resistivity and stimulate a crossover from metallic to insulating behavior which may be related to a distortion of the Fermi surface, but the peak is still alive. To give more insight into this anomalous peak, the following MR measurements are carried out at three typical temperatures ($T = 2$, 65 and 100 K) as marked in the main panel in Fig. 1(b).

As shown in Figs. 1(c)–1(f), at $T = 2$, 65 and 100 K, the MR is measured by tilting the magnetic field from perpendicular ($\theta = 0°$) to parallel ($\theta = 90°$) to the electric current direction. The insets zoom in on the lower MR parts and depict the corresponding measurement configurations. At $T = 2$ K (see Fig. 1(c)), the MR exhibits obvious Shubnikov-de Haas (SdH) oscillations with a very low frequency of ∼1 T in the low field range, which result from the depopulation of the Landau levels $N = 3$, 2 and 1, suggesting the existence of a very small concentration of light carriers. Beyond this quantum limit ($B \sim 2$ T), the MR increases parabolically with B and reaches 4000% at 9 T. We also find that the quantum limit depends on the title angle θ, and the MR is suppressed remarkably as θ is increased. We do not observe a negative MR at $\theta = 90°$. In contrast to the case at $T = 2$ K, in the inset of Fig. 1(d), a clear negative

MR at $T = 65\,\mathrm{K}$ is detected in the parallel electric and magnetic fields, hinting at the presence of the chiral anomaly of Weyl fermions. Remarkably, the MR decreases monotonously and tends to saturation with increasing the magnetic field, indicating the high quality of the sample. Furthermore, we note that the MR curve appears to have a broad cusp-like depression, as shown in the main panel of Fig. 1(d), which is corresponding to the so-called WAL observed commonly in graphene and topological insulators,[45–47] in which Dirac fermions dominate the magneto-electric transport. Measurements are also implemented by tilting the magnetic field with respect to the (010) facet but keeping the field perpendicular to the current (see Fig. 1(e)). As is expected, the WAL behavior is free from effect, but no trace of negative MR phenomenon has been detected. This adds evidence that the negative MR originates from the chiral term $\boldsymbol{E}\cdot\boldsymbol{B}$.

When the temperature increases to 100 K (see Fig. 1(f)), both the negative MR and the WAL disappear. Namely, the WSM state is destroyed by further increasing the temperature. The whole process presented in Figs. 1(c)–1(f) can be interpreted as a temperature-induced changing of the topological band structure of $HfTe_5$, which generates non-trivial Dirac-like linear dispersion at around $T_p \sim 65\,\mathrm{K}$. The extrinsic magnetic field breaks the time-reversal symmetry and degenerates the Dirac node to a pair of Weyl nodes. In the following we discuss in detail the unusual evolution of the negative MR and WAL behaviors when the magnetic field is parallel and perpendicular to the current.

Figures 2(a) and 2(b) present the MR measured at typical temperatures in parallel electric and magnetic fields. At 2 K, the value of MR is positive in the whole range of the applied magnetic fields. Remarkably, there is a negative trend with increasing the temperature, and eventually the MR falls to -30% at $T = 60\,\mathrm{K}$ and $B = 9\,\mathrm{T}$. This response to temperature change is opposite to that observed in the 3D DSMs/WSMs, such as TaAs, Na_3Bi, and $Bi_{1-x}Sb_x$.[21,41,44] Upon further increasing the temperature, the negative MR is gradually suppressed, and the positive MR appears again above 100 K. When a perpendicular magnetic field is applied, as shown in Figs. 2(c) and 2(d), while the WAL effect is less affected by lowering temperature, indicating that the topological surface states are remarkably robust at low temperature region. Above T_p, as the temperature increases, the cusps are broadened and finally disappear due to the continuous decrease of the phase coherent length. Overall, one can attribute these unique phenomena to the formation of a 3D DSM state at around T_p, which has been proposed to appear in the critical point of topological quantum phase transition (TQPT) between two different topological phases through accidental band crossing.[26] For example, by fine tuning the chemical composition in $BiTl(S_{1-\delta}Se_\delta)_2$, a 3D DSM state has been realized at the critical point of the TQPT.[30]

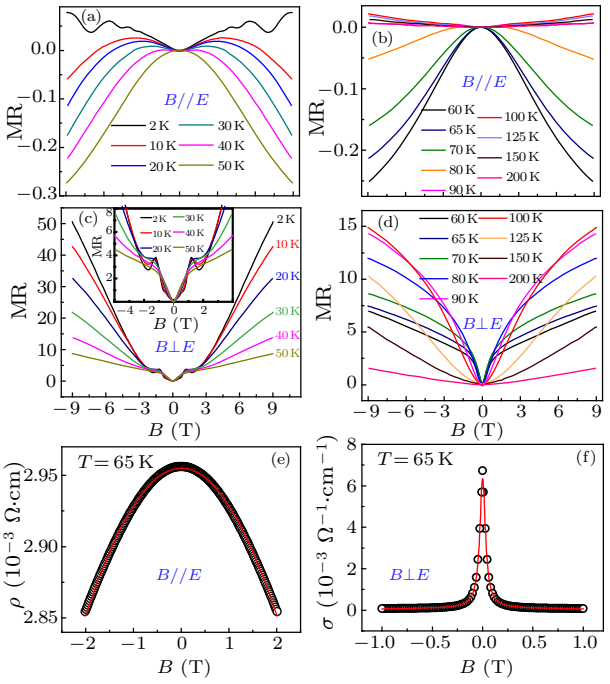

Fig. 2. (a, b) Magneto-resistivity at different temperatures with the applied magnetic field parallel to the electric current. (c, d) Magneto-resistivity at different temperatures with the applied magnetic field perpendicular to the electric current. Inset shows MR with expanded scale. (e, f) Negative MR ($\boldsymbol{B}//\boldsymbol{E}$) and WAL effect ($\boldsymbol{B}\perp\boldsymbol{E}$) at 65 K in weak magnetic fields. The black circles and the red line represent the experimental results and theoretical fitting, respectively. All these signify the appearance of the chiral electrons with Berry's phase of π.

The effects of the negative MR and WAL on transport properties of WSM can be described in a general formula[21,44]

$$\sigma(B) = (1 + C_W B^2)\cdot\sigma_{WAL} + \sigma_N, \tag{1}$$

where

$$\sigma_{WAL} = \sigma_0 + a\sqrt{B}, \tag{2}$$

$$\sigma_N^{-1} = \sigma_0^{-1} + A\cdot B^2, \tag{3}$$

σ_0 is the zero field conductivity, and C_W is a positive parameter which originates from the topological $\boldsymbol{E}\cdot\boldsymbol{B}$. Such a topological term will generate chiral current in the non-orthogonal magnetic and electric fields. Here σ_{WAL} and σ_N are from the WAL effect and the normal nonlinear band structures around the Fermi level, respectively. At $\theta = 90°$, the contribution from the σ_{WAL} term can be considered as a constant σ^0_{WAL}, since the samples are thin ribbon-like quasi-two-dimensional single crystals, and C_W is a nonzero value. Then, in the weak field region, the chiral conductivity derived from Eq. (1) is expressed by[44]

$$\sigma^{chiral} = (1 + C_W B^2)\cdot\sigma^0_{WAL}. \tag{4}$$

In contrast, at $\theta = 0°$, the topological $\boldsymbol{E}\cdot\boldsymbol{B}$ term is zero, and the contribution from $C_{\rm W}$ vanished. However, the effect of WAL on the conductivity cannot be ignored. As a consequence, Eq. (1) is rewritten as

$$\sigma(B) = (\sigma_0 + a\sqrt{B}) + (\rho_0 + A\cdot B^2)^{-1}. \quad (5)$$

The measured negative MR ($\theta = 90°$) and WAL ($\theta = 0°$) data at $T = 60\,\mathrm{K}$ are fitted with Eqs. (4) and (5), respectively. As shown in Figs. 2(e) and 2(f), the black circles represent the experimental results and the red lines depict the theoretical fittings. The fittings show excellent agreement between the experimental data and theoretical curves with the parameters of $\sigma_0 = 338.4\,\Omega^{-1}\mathrm{cm}^{-1}$, $C_{\rm W} = 3.04\,\mathrm{T}^{-2}$, $A = 1.38\times10^5\,\Omega\cdot\mathrm{cm}\mathrm{T}^{-2}$ and $\rho_0 = 163\,\Omega\cdot\mathrm{cm}$. This confirms that the negative MR and WAL at around $T_{\rm p}$ originate from the chiral Weyl fermions, signalling a temperature-tuned DSM state in $HfTe_5$.

Magnetic-field-dependent Hall resistivity ρ_{xy} of $HfTe_5$ at different temperatures is studied and presented in Fig. 3. As shown in Fig. 3(a), at high temperatures, the positive slopes of Hall resistivity indicate that the holes dominate the main transport process. With the temperature down to 80 K, however, both the slopes and the values of Hall resistivity change signs in low fields, implying the carriers dominating the conduction mechanism transformed to electron-type. All these are consistent with multiple hole- and electron-like carriers as observed in TaAs.[21] For a simple two-carrier model, the Hall conductivity σ_{xy} is expressed as[48]

$$\sigma_{xy} = \left[a_1 n_1 \mu_1^2 \frac{1}{1+(\mu_1 B)^2} - a_2 n_2 \mu_2^2 \frac{1}{1+(\mu_2 B)^2}\right] eB, \quad (6)$$

where n_1 (n_2) and μ_1 (μ_2) represent the concentration and mobility for two kinds of carriers, respectively. We should note that the 'two kinds of carriers' may not only represent the coexistence of electrons and holes, but also signal the possibility of the existence of two kinds of electrons (or holes) with distinct dispersion relations. This resorts to the sign of $a_1 n_1$ and $a_2 n_2$, in which $a_1 = -1$ (or $+1$) correspond to electron-carriers (or hole-carriers), and $a_2 = -1$ (or $+1$) correspond to hole-carriers (or electron-carriers), respectively. Figure 3(b) presents the Hall conductivity σ_{xy} (solid lines) and the nicely fitting results (dotted lines) at several temperatures. Using the fitting parameters, we extract the Hall mobility and carrier concentrations. As shown in Fig. 3(c), the two kinds of Hall mobility exhibit distinct behaviors with respect to temperatures. Here μ_2 is nearly constant in a wide temperature range from low to high temperatures. However, with decreasing the temperature, especially below 65 K, μ_1 increases dramatically and reaches up to $2.4\times10^5\,\mathrm{cm}^2\mathrm{V}^{-1}\mathrm{s}^{-1}$ at 2 K. The high carrier mobility is one of the hallmarks of Dirac or Weyl fermions.[21,49] The unusual behavior around 65 K can be further understood by analyzing the carrier concentrations. Figure 3(d) can be intuitively divided into four different parts. As is shown, both kinds of carriers are hole-type at higher temperatures, and the concentrations decrease remarkably with decreasing the temperature. At around 110 K, the carriers are related to μ_2 changing from hole-type to electron-type, which corresponds to the metal-insulator transition in resistivity. Notably, the carriers are related to μ_1 changing their type near 65 K, signaling the temperature-tuned changing of the Fermi surfaces at this temperature. The inset of Fig. 3(c) shows the temperature dependence of Hall coefficient $R_{\rm H}$ calculated at $B = 1.1\,\mathrm{T}$. It is interesting to note that $R_{\rm H}$ sharply reverses its sign at around $T_{\rm p} \sim 65\,\mathrm{K}$, which is very different from that of other multiple band systems, in which $R_{\rm H}$ changes sign gradually when the dominant carrier type switches.[21,49] This observation confirms further the occurrence of the band recombination due to a topological phase transition in $HfTe_5$.

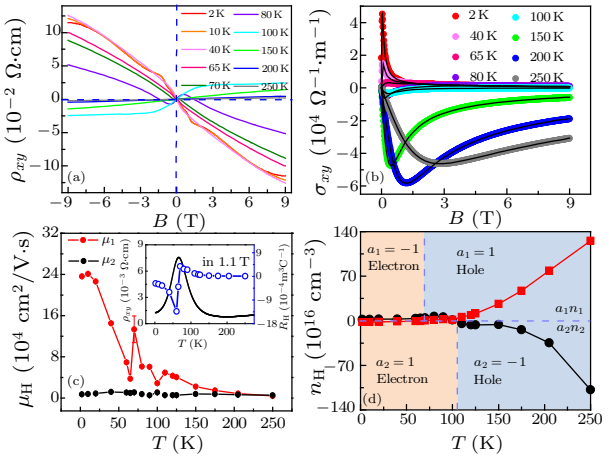

Fig. 3. (a) Hall resistivity measured at various temperatures from 2 to 250 K. (b) Magnetic field dependence of σ_{xy} at various temperatures. The dotted and the solid lines represent the measuring and the fitting data, respectively. There is a large error in the data fitting for 65 K. (c) Temperature dependence of carrier mobility μ_1, and μ_2 for different carriers deduced by the two-carrier model. Inset: the large resistivity peak at zero magnetic field and Hall coefficient obtained by fitting the experimental data below 1.1 T. (d) Temperature dependence of carrier densities n_1 and n_2 for different carriers deduced by the two-carrier model.

In Ref. [38], the single layer of $ZrTe_5$ or $HfTe_5$ has been proposed to be a 2D TI with large band gap. Therefore, the 3D $HfTe_5$ can be looked on as the stacking of the 2D TIs along b-axis with quite weak van der Waals interaction. The band dispersion along b-axis might lead to band inversion if the interlayer coupling is strong enough. This will lead to a TQPT from 3D weak TI to strong TI. The first-principles calculation indicates that both $ZrTe_5$ and $HfTe_5$ are at the

vicinity of such TCP.[38] In Figs. 4(a) and 4(d), the interlayer distance is 5% longer than the experimental value (7.22 Å) and the calculated band structure indicates that there is no band inversion along the layer stacking direction Γ–Z. It is a weak TI with Z_2 indices of (0; 010). With slightly reducing the interlayer distance by 2.5%, the band gap closes at TCP in Figs. 4(b) and 4(e). It reopens in Figs. 4(c) and 4(f) with the interlayer distance being the experimental value. It is a strong TI with Z_2 indices of (1; 010). At the TCP, the Dirac cone-like band dispersion at Γ can be looked on as a class-2 DSM.[27]

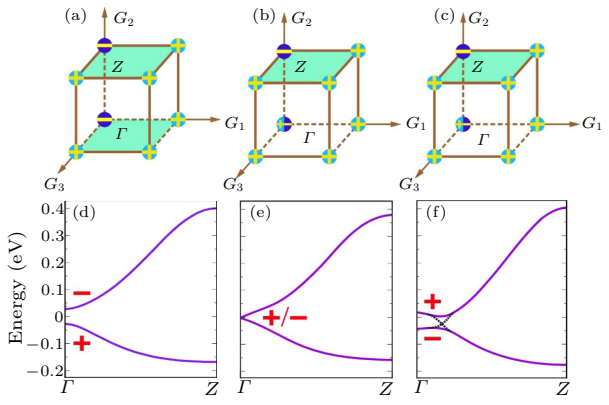

Fig. 4. Topological quantum phase transition driven by the interlayer coupling. The parity configuration (+ means even parity and − means odd one) at eight time-reversal invariant momenta (TRIM) in (a) weak TI phase with interlay distance of 5% longer than the experimental value, (b) TCP with interlayer distance of 2.5% longer, and (c) strong TI phase with experimental value, respectively. The corresponding band dispersion along layer stacking direction Γ–Z is shown in (d)–(f) in order of increasing the interlayer coupling. (f) The band crossing (black dotted line) in the case without the spin–orbit coupling is open when the SOC is considered.

Combining the theoretical and experimental results, the mystery of the anomalous resistivity in $HfTe_5$ that has perplexed researchers for more than 30 y has been solved. At high temperatures, the bulk band gap is opened and $HfTe_5$ exhibits the semiconducting behavior. With the sample cooling, the bulk band gap goes to zero at a critical temperature T_p and thereafter the surface state dominates the electronic transport properties, which thus leads to a pronounced resistivity peak at around T_p.

In summary, we have found a temperature-induced change of the topological band structure in $HfTe_5$ as evidenced by magneto-transport measurements. Remarkably, in the critical point of the TQPT between the weak and strong TI phases, a 3D Dirac semimetal state appears through accidental band crossing at the critical temperature T_p, manifested by the observation of a large negative MR and WAL effect. By approaching to critical point, the bulk band gap goes to zero and leads to a pronounced resistivity peak. Our work gives a reasonable interpretation of the long-standing confusion of the anomalous resistivity peak in $HfTe_5$.

We wish to thank Lu Li for fruitful discussion and helpful comments.

References

[1] Qi X L et al 2011 *Rev. Mod. Phys.* **83** 1057
[2] Hasan M Z et al 2010 *Rev. Mod. Phys.* **82** 3045
[3] Weng H M et al 2015 *Adv. Phys.* **64** 227
[4] Weng H M et al 2014 *MRS Bull.* **39** 849
[5] Fu L 2011 *Phys. Rev. Lett.* **106** 106802
[6] Hsieh T H et al 2012 *Nat. Commun.* **3** 982
[7] Dziawa P et al 2012 *Nat. Mater.* **11** 1023
[8] Tanaka Y et al 2012 *Nat. Phys.* **8** 800
[9] Dzero M et al 2010 *Phys. Rev. Lett.* **104** 106408
[10] Lu F et al 2013 *Phys. Rev. Lett.* **110** 096401
[11] Weng H M et al 2014 *Phys. Rev. Lett.* **112** 016403
[12] Xu N et al 2014 *Nat. Commun.* **5** 4566
[13] Young S M et al 2012 *Phys. Rev. Lett.* **108** 140405
[14] Wang Z J et al 2012 *Phys. Rev.* B **85** 195320
[15] Wang Z J et al 2013 *Phys. Rev.* B **88** 125427
[16] Liu Z K et al 2014 *Science* **343** 864
[17] Liu Z K et al 2014 *Nat. Mater.* **13** 677
[18] Weng H M et al 2015 *Phys. Rev.* X **5** 011029
[19] Wan X G et al 2011 *Phys. Rev.* B **83** 205101
[20] Xu G et al 2011 *Phys. Rev. Lett.* **107** 186806
[21] Huang X C et al 2015 *Phys. Rev.* X **5** 031023
[22] Lv B Q et al 2015 *Phys. Rev.* X **5** 031013
[23] Lv B Q et al 2015 *Nat. Phys.* **11** 724
[24] Xu S Y et al 2015 *Science* **349** 613
[25] Lu L et al 2015 *Science* **349** 622
[26] Murakami S 2011 *Physica* E **43** 748
[27] Yang B J et al 2014 *Nat. Commun.* **5** 4898
[28] Bahramy M S et al 2012 *Nat. Commun.* **3** 679
[29] Xi X et al 2013 *Phys. Rev. Lett.* **111** 155701
[30] Xu S Y et al 2011 *Science* **332** 560
[31] Sato T et al 2011 *Nat. Phys.* **7** 840
[32] Brahlek M et al 2012 *Phys. Rev. Lett.* **109** 186403
[33] Wieting T J et al 1980 *Bull. Am. Phys. Soc.* **25** 340
[34] Disalvo F J et al 1981 *Bull. Am. Phys. Soc.* **26** 449
[35] Disalvo F J et al 1981 *Phys. Rev.* B **24** 2935
[36] Okada S et al 1982 *J. Phys. Soc. Jpn.* **51** 460
[37] McIlroy D N et al 2004 *J. Phys.: Condens. Matter* **16** L359
[38] Weng H M et al 2014 *Phys. Rev.* X **4** 011002
[39] Hosur P et al 2013 *Comptes Rendus Phys* **14** 857
[40] Son D T et al 2013 *Phys. Rev.* B **88** 104412
[41] Xiong J et al 2015 *Science* **350** 413
[42] Parameswaran S A et al 2014 *Phys. Rev.* X **4** 031035
[43] Potter A C et al 2014 *Nat. Commun.* **5** 5161
[44] Kim H J et al 2013 *Phys. Rev. Lett.* **111** 246603
[45] Wu X S et al 2007 *Phys. Rev. Lett.* **98** 136801
[46] Liu M H et al 2012 *Phys. Rev. Lett.* **108** 036805
[47] Ishiwata S et al 2013 *Nat. Mater.* **12** 512
[48] Ashcroft N W et al 1976 *Solid State Physics* (New York: Holt, Rinehart and Winston)
[49] Liang T et al 2014 *Nat. Mater.* **14** 280